

## Effects of Particle Size and Electrical Resistivity of Filler on Mechanical, Electrical, and Thermal Properties of Linear Low Density Polyethylene–Zinc Oxide Composites

Filiz Ömürlü Özmişçi, Devrim Balköse

İzmir Institute of Technology, Chemical Engineering Department Gülbahçe köyü, Urla-İzmir 35430, Turkey

Correspondence to: F. Ö. Özmişçi (E-mail: filizozmishci@iyte.edu.tr)

**ABSTRACT:** The effects of particle size and electrical resistivity of zinc oxide (ZnO) on mechanical properties, electrical and thermal conductivities of composites made with linear low density polyethylene (LLDPE) were investigated. Micron sized (mZnO), submicron sized (sZnO), and nano sized (nZnO) powders having resistivities of  $1.5 \times 10^6$ ,  $1.5 \times 10^9$ , and  $1.7 \times 10^8$  were used to prepare composites with 5–20 vol % filler. The tensile strength was lowered and the modulus of elasticity of the composites was increased with ZnO addition. Rather than the particle size of the ZnO, its initial resistivity and aspect ratio affected the resistivity of composites. The resistivity of the LLDPE was lowered from  $2.3 \times 10^{16} \Omega \text{ cm}$  down to  $1.4 \times 10^{10} \Omega \text{ cm}$  with mZnO addition. Thermal conductivity of the composites was increased with ZnO addition 2.5–3 times of the polymer matrix. The composites can be used for electrostatically dissipating and heat sink applications due to their decreased electrical resistivity and increased thermal conductivity.

© 2013 Wiley Periodicals, Inc. *J. Appl. Polym. Sci.* 000: 000–000, 2013

**KEYWORDS:** composites; properties and characterization; surfaces and interfaces; morphology

Received 14 February 2013; accepted 20 April 2013; Published online 00 Month 2013

DOI: 10.1002/app.39433

### INTRODUCTION

Polymeric materials are generally insulating materials and normally used as insulators in electric and electronic applications and tend to accumulate electrostatic charge.<sup>1</sup> Electrostatic charge can damage highly sensitive electronic components or cause materials to ignite and gases to explode. A practical solution to overcome these problems is to lower the resistivity of the polymer. Adding antistatic agents is one of the methods lowering the resistivity of the polymer however, soap like molecules of antistatic agents diffuse to the surface of the material and only the surface resistivity drops. To lower the electrical resistivity, addition of conductive fillers (metals or metal oxides) is another method suggested in the literature.<sup>2–4</sup>

ZnO has a hexagonal crystal structure and composed of tetrahedrally coordinated  $\text{O}^{2-}$  and  $\text{Zn}^{2+}$  ions and a large exciton binding energy of 60 meV. ZnO is used in many applications in improving the optical, electrical, and mechanical properties of devices, in photovoltaic solar cells, as photoconductive ingredient, in rubber industry, as pigments and coatings, light-emitting diodes, transparent transistor, memory devices, varistors, ceramics, catalysts, flame retardants, and as an additive material in cosmetics and the polymeric matrices.<sup>5–7</sup>

The electrical conductivity behavior of a composite material is related to the theory of percolation. The electrical conductivity of the composite material behaves like the polymer matrix up to the

threshold value. At or above the threshold value, the electrical properties of the composite change and the overall behavior approaches the electrical properties of filler rather than matrix. This change is due to the decrease in the interparticle distance of the filling materials.<sup>8,9</sup> The percolation threshold value and the electrical conductivity of the composites depends on many factors such as filler characteristics (size, shape, aspect ratio, and morphology), processing conditions, spatial distribution of the filler within the matrix, volume fraction of the filler, crystallization character of the polymer matrix, the interaction between polymer and filler surfaces, and the contact resistance between particles.<sup>9–15</sup> Gokturk et al.<sup>15</sup> showed that the fiber and flake-shaped fillers were more effective in decreasing electrical resistivity than spherical powders.

The surface properties of the filler and polymer also have a significant effect on the conductivity of the composites. Surface free energies of the filler and the matrix influence the interaction between two materials, i.e., how well the polymer wets the surface of the filler. Thus polymers cannot wet the inorganic material if its surface energy is higher than the polymer and an adequate surface treatment of the filler is necessary.<sup>15–18</sup>

Hong et al.<sup>18</sup> studied addition of nanosized and micron sized ZnO to low molecular weight polyethylene. The percolation threshold value for ZnO–polyethylene composites were found

approximately at 30 vol % and addition of 40 vol % ZnO decreased the resistivity to  $10^{11} \Omega \text{ cm}$ .<sup>18</sup> In another investigation, the particle size effect was studied by using nano and micron sized ZnO particles and the electrical resistivity was found at the order of  $0.3 \times 10^{13} \Omega \text{ cm}$  after the addition of 60 vol % ZnO.<sup>19</sup> In contrast, Hong et al.<sup>18</sup> reported the lowest resistivity as  $10^9 \Omega \text{ cm}$  upon the addition of 30 vol % ZnO. In fact Hong et al. studied ZnO particles and linear low density polyethylene (LDPE) composites to investigate the particle size affect. Micron sized (300 nm) and nanosized (49 and 24 nm) powders were used as fillers in their study. The percolation limit decreased as the particle size of zinc oxide was decreased. When the interparticle distance was decreased to below 40 nm, tunneling began to occur. The percolation onset occurred at a lower volume fraction as the particle size was decreased, due to decrease in interparticle spacing. The neat polymer volume resistivity was  $10^{19} \Omega \text{ cm}$  and the lowest volume resistivity found was  $10^9 \Omega \text{ cm}$  for 24 nm powder at above 30 vol %.<sup>18</sup>

In another approach, micron sized and nanosized particles will penetrate the amorphous regions of the PE but not the crystalline parts. Since the crystalline part has a negative electron affinity, electron transport through PE occurs mainly through the amorphous regions, and over the surfaces of the crystalline regions. The conductivity decrease in composites loaded with nanosized ZnO particles modified with a hyperdispersant was due to the reduction of the electronic carrier mobility in the amorphous regions.<sup>20</sup>

Filler/polymer composites thermal conductivity which is path dependent is a bulk property unlike electrical conductivity. In percolation threshold value, the electrical conductivity raises about 10 orders of magnitude over a small range of concentration where the fillers get close enough to conduct current with little resistance.<sup>21</sup> Kumlutaş and Tavman studied the thermal conductivity of polypropylene with 30% addition of talc from 0.27 up to 2.5 W/mK. The same matrix material containing the same volume fraction of copper particles had a thermal conductivity of only 1.25 W/mK. However; the thermal conductivity of copper particles were approximately 40 times greater talc particles which is directly due to a complete interconnectivity achieved from talc particles in polypropylene while copper particles show a very poor interconnectivity.<sup>22</sup>

LLDPE was used in packaging and coating industry to make thinner films than low density polyethylene. Recent articles nicely illustrated how particle size, filler geometry, and crystallinity affected the electrical resistivity of the ZnO and LLDPE composites and the importance of interparticle distance.<sup>19,20</sup> However, the possibility of ZnO fillers having different sizes could have different electrical resistivities was not considered in these studies.<sup>19,20</sup> Composites having a very low amount of ZnO was examined for mechanical properties.<sup>19,20,23</sup> However, higher filler loading was necessary for making polyethylene thermally conductive.<sup>24</sup> The main application for thermally conductive polymers was heat sinks. Several conductive fibers such as carbon fibers, nickel-coated graphite fibers, copper fibers, brass fibers, stainless steel fibers, metal oxides, etc., have been used to overcome these deficiencies.<sup>8,16</sup>

Thus studying the effects of ZnO on the mechanical and electrical properties of LLDPE composites with high ZnO loading was

necessary. In this study, the effects ZnO particles having different initial resistivity values on crystallinity, contact angle, surface roughness, mechanical properties, electric resistivity, and thermal conductivity of the LLDPE–ZnO composites were aimed to be investigated.

## EXPERIMENTAL

### Commercial ZnO Powders and Polyethylene

Three commercial ZnO powders having particle sizes in micrometer (mZnO), submicrometer (sZnO), and nanosize (nZnO) range were supplied by Ege Kimya Co. (mZnO) and Aldrich (sZnO, nZnO), respectively. The particle sizes of the powders were determined by Zeta Sizer (Malvern Instruments 3000 HSA). Linear low density polyethylene (LLDPE) from Aldrich with melt flow index: 1.0 g /10 min (190°C/2.16 kg) was used as a matrix material.

### Composite Preparation

ZnO and polymer mixing process was performed in a torque rheometer (Haake Polydrive Rheomixer R600/610) at 50 rpm speed at 160°C and for 20 min. The blended materials were then uniaxially pressed at 6800 kg force at 150°C with 10 min hold time in a hot press (Carver) to have sheets with 15 cm × 15 cm × 0.1 cm dimensions.

mZnO and sZnO–polymer composites were prepared having 0, 5, 10, 15, and 20 vol % ZnO in polyethylene. Polymeric composites with LLDPE matrix were prepared only for 5, 10, and 15 vol % nZnO, since wetting problems were present for 20 vol % ZnO in LLDPE.

### Characterization of ZnO Powders and the Composites

**Crystal Structure.** Crystal structures of the ZnO powders and the composites were determined by X-ray diffractometer (Phillips X'Pert diffractometer, Cu K $\alpha$  radiation).

**Electrical Resistivity Measurement.** ZnO pellets having 2.5 cm diameter and 2 mm were prepared from the ZnO powders by pressing under 10 MPa pressure. Silver contacts were formed by thermal evaporation of silver on both surfaces of the ZnO pellet for the resistivity measurement. The volumetric resistivity of the pellet was determined by sweeping the potential between  $-50 \text{ V}$  and  $+50 \text{ V}$  and recording  $I$ – $V$  data with Keithley 2420.

Volume electrical resistivity of the composites was measured according to ASTM D257 by using Keithley 6517A Electrometer/High Resistance meter connected to 8009 Resistivity Text Fixture sample holder (Keithley 6517-A manual, 2004). The voltage was changed alternatively between  $-50$  and  $+50 \text{ V}$  and the current was measured. At the end of the test (8 readings), an average data was given as the resistivity value.

**Thermal Conductivity of the Composites.** The thermal conductivity of the samples was measured by hot wire method using quick thermal conductivity meter KEM QTM-500.

**Surface Area of ZnO Powders.** The N<sub>2</sub> adsorption/desorption analysis were performed to determine the surface area of the mZnO and sZnO powders (ASAP Micromeritics 2000).

**Contact Angle of Water on Powders and Films.** ZnO powders were dry pressed to obtain pellets with 2.5 cm diameter and

2–3 mm thickness. They were sintered at 1100°C and their surfaces were polished with diamond suspension and 1100 SiC paper. Their contact angle of water was measured with Krüss-G10 goniometer. Surface roughness of the sintered pellets and the polymer films were determined by Mitutoyo Surface Profilometer, SJ-301. Contact angle of the composites were measured five times using Attension theta optical tensiometer with attached camera of KSU CAM 101 and average data were given as the contact angle.

**Morphology of the Composites.** The morphology of composites was characterized by using SEM (Philips XL-30S FEG). Fracture surfaces obtained by breaking of composites after immersing in liquid N<sub>2</sub> (77 K) were examined using SEM.

**Tensile Tests.** The tensile behavior of the samples were measured by using Shimadzu AG-I 25 kN tensile tester at 50 mm/min stretching rate at room temperature according to ASTM standard 638. For this purpose, dogbone samples (10 cm length) were cut from the composite plates by using Ceast automatic die punch.

## RESULTS AND DISCUSSION

### Characterization of ZnO Particles

The X-ray diffraction diagrams of the mZnO, sZnO, and nZnO were identical to each other. In Figure 1, curve 1 is the X-ray diffraction diagram of mZnO. The peaks at  $2\theta$  values of 31.9°, 34.5°, 36.2°, 47.5°, 56.5°, 62.8°, 67.9°, and 69.3° are identical with the peaks at the XRD pattern of ZnO powder in JCPDS Card No: 79-0207.<sup>25</sup> Thus crystal structure of mZnO, sZnO, and nZnO is the typical wurtzite structure of bulk ZnO. Table I clearly represents the particulate dimensions of ZnO powders. The crystal sizes of the ZnO powders reported in Table I were calculated using Scherrer equation for the diffraction peak at  $2\theta$  value of 34.25° for (002) planes. Figure 2 provides SEM micrographs and particle size distributions of ZnO particles determined by Zeta Sizer. The morphologies of mZnO, sZnO, and nZnO powders were all different from each other as seen in Figure 2. The particles of mZnO had different shapes such as rod, sphere and tripod shaped particles which points to their polycrystalline nature [Figure 2(a)]. sZnO particles were mostly bar-like shaped as seen in Figure 2(b). On the other hand, nZnO particles were nearly in spherical shapes [Figure 2(c)]. SEM pictures of the particles indicated that particles of mZnO had higher aspect ratio value (4.35) than those of nZnO (1.96) and sZnO (2.29).

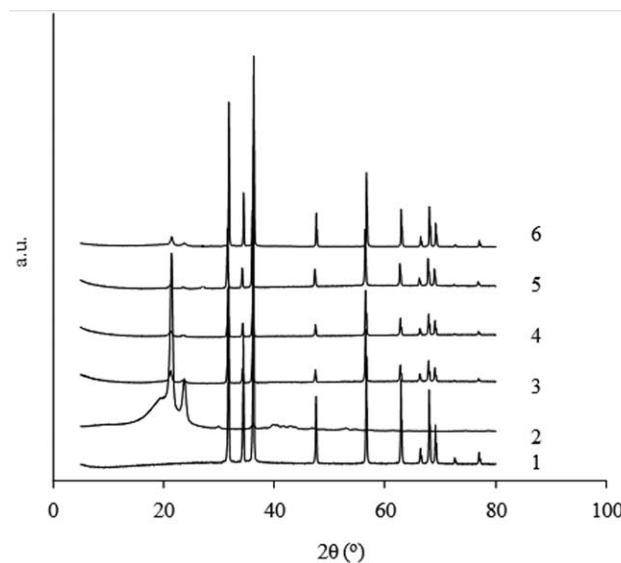


**Figure 1.** X-ray diffraction diagrams of (1) mZnO, (2) LLDPE, (3) 5 vol % mZnO, (4) 10 vol % mZnO, (5) 15 vol % mZnO, (6) 20 vol % mZnO–LLDPE composites.

Table I reports the properties of the ZnO powders used in the experiments. The surface area of the powders increased from 1.5 to 20 m<sup>2</sup>/g as their particle size decreased as shown in Table I. The SEM size, mean particle size from zeta sizer, and crystal size differ due to the polydisperse nature of the powders as well. The size of the particles determined by zeta sizer was considerably larger than the crystallite size determined by X-ray diffraction indicating polycrystalline nature of the particles. Figure 2(d–f) shows the particle size distribution of the powders determined by the zeta sizer. The mZnO had a broad particle size distribution between 0.9–9 μm and the average particle size was determined as 3860 nm [Figure 2(d)]. mZnO particle size was determined as 416 nm by the X-ray diffraction. On the other hand, sZnO had a bidisperse distribution with 10% of the particles in 10–100 nm range and 90% of them 100–1100 nm range [Figure 2(e)]. The average particle size of sZnO was determined as 752 nm by zeta sizer and its crystal size was 238 nm. The nZnO had the narrowest particle size distribution (between 300–400 nm) compared to that of mZnO and sZnO and the average size was determined as 378 nm by zeta sizer [Figure 2(d)]. The crystal size of the nZnO determined as 203 nm by X-ray diffraction (Table I).

**Table I.** Properties of ZnO

Type of ZnO	Mean particle size <sup>a</sup> (nm)	Crystal size <sup>b</sup> (nm)	Aspect ratio from SEM	Surface area (m <sup>2</sup> /g)	Contact angle (°)	Surface roughness (μm)	Volume resistivity (Ω cm)
mZnO	3860	416	4.35	1.5	47	0.02	1.5 × 10 <sup>6</sup>
sZnO	752	238	1.96	10.1	45	0.07	1.5 × 10 <sup>9</sup>
nZnO	378	203	2.29	20.0	38	0.20	1.7 × 10 <sup>8</sup>

<sup>a</sup> Measured with zeta sizer.

<sup>b</sup> Calculated from X-ray diffraction peak of the 0 0 2 planes at  $2\theta$  34.25°.

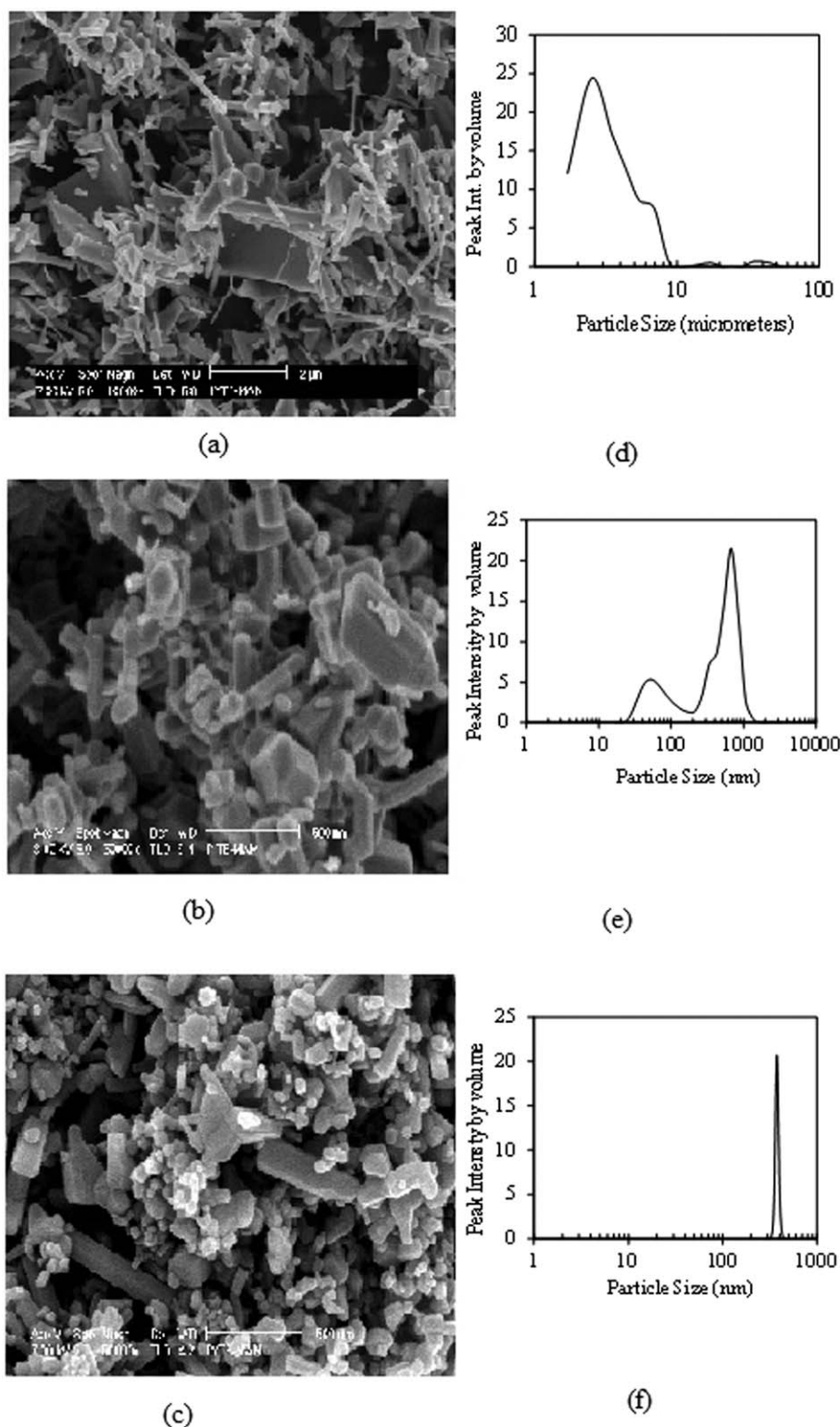


**Figure 2.** SEM micrographs (a) mZnO (b) sZnO and (c) nZnO powders (Scale bar 2 μm, 500 nm, and 500 nm, respectively) and particle size distribution of (d) mZnO (e) sZnO and (f) nZnO powders determined by the zeta sizer.

The volumetric resistivity of mZnO ( $1.5 \times 10^6 \Omega \text{ cm}$ ) was lower than that of nZnO ( $1.5 \times 10^9 \Omega \text{ cm}$ ) and sZnO ( $1.7 \times 10^8 \Omega \text{ cm}$ ) powders (Table I). Since the powders were obtained

by different methods, they have different impurities acting as dopants in their conductivity. mZnO being a commercial powder had impurities making its resistivity low.

The surface roughness of the pellets were also measured and given in Table I. There should be no error in measuring contact angle due to the surface roughness of the materials since the roughness was found to be very low (0.02–0.2  $\mu\text{m}$ ). The contact angle of water on the ZnO pellets was in the range of 38–47° as reported in Table I and indicated that all the powders were hydrophilic. However, nZnO had the lowest contact angle, 38° and it was more hydrophilic than mZnO and sZnO.

### Crystallinity of the LLDPE in Composites

In the XRD pattern of LLDPE in Figure 1, curve 2 one dominant fairly sharp peak at  $2\theta$  value of 21.4° for (1 1 0) planes and a weak broad peak at  $2\theta$  value of 23.6° for (2 2 0) planes and a weak, broad third peak centered at 19.5° for amorphous regions<sup>26</sup> are present. It was clear from the relative areas under these peaks that the polymer sample produced in plate form after solidification from the melt become highly crystalline. The composites possess typical crystal peaks of ZnO and also increasing ZnO content increases the intensity of the peaks as shown in Figure 1. The intensity of the crystal and amorphous peaks of LLDPE was much lower than the intensity of the ZnO peaks. However, it was possible to calculate the crystallinity of LLDPE in each composite from the areas of the crystalline peaks at  $2\theta$  values of 21.4° and 23.6° and amorphous peak at 19.5° in the X-ray diffraction diagrams. The following procedure was adopted to calculate the total crystalline fraction and contributions from each crystalline phase. From the iterative peak-fit procedure, the crystalline peaks, and the amorphous peaks were isolated. Total crystallinity of various samples was calculated by using the following eq. (1).

$$\% \text{ Crystallinity} = W_C / (W_C + W_a) \times 100 \quad (1)$$

$W_C$  is the integral area of peaks of crystalline phase and  $W_a$  is the integral area of peaks of amorphous phase. The crystallinity of the mZnO–LLDPE and sZnO–LLDPE composites found from XRD is shown in Figure 3 as a function of the volume fraction of the filler. Crystallinity of the LLDPE matrix was essentially affected by ZnO powder addition. The crystallinity of the composites increased with their ZnO content. Crystallinity value of the composites increased from 44% up to 60% for mZnO and 54% for sZnO by ZnO addition up to 20 vol %. Thus the particle size difference did not have a significant effect on the crystallinity of LLDPE.

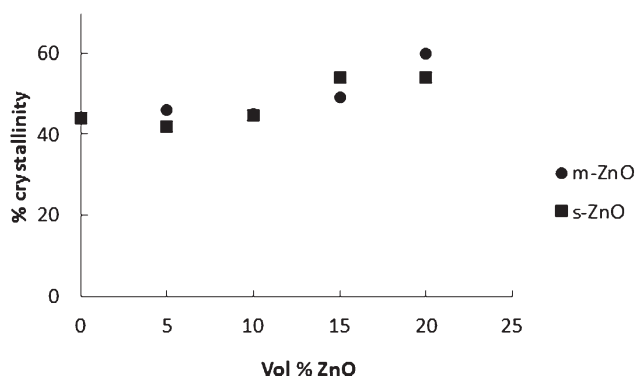


Figure 3. X-ray crystallinity versus vol % of ZnO in the composites.

### Dispersion of ZnO in Composites

Representative SEM images of the fracture surfaces of sZnO loaded composites are given in Figure 4. Particles of sZnO appear as white features against dark background due to the polymer. In Figure 4, almost all particles were evenly distributed in the continuous phase (LLDPE phase). In some of the regions, there were voids (gaps) present between the particles and the polymer. In Figure 4(d) for 20 vol % nZnO composite, a spider net like feature was formed by plastic deformation of polymer phase during fracture. There were clusters of several particles. This could be attributed to the dispersion and wetting problem in the interface between ZnO and LLDPE. The wetting and dispersion problem was due to the poor compatibility between the polymer and filler. Similarity of filler and matrix phase surfaces is necessary for a good adhesion between them. Thus Hansen solubility parameters of the polymer and ZnO were compared in this study to predict their compatibility.  $\delta_D$ ,  $\delta_P$ ,  $\delta_H$ , and  $R_o$  values for LDPE were reported as 16.3, 5.9, 4.1, and 8.4, respectively. On the other hand, ZnO has 16.9, 7.8, and 13.2 for Hansen Solubility Parameters  $\delta_D$ ,  $\delta_P$ ,  $\delta_H$  values, respectively.<sup>27</sup> The  $R/R_o$  value found from these values was 1.13 which is greater than 1. If  $R/R_o$  is greater than 1 the solid surface and the polymer do not have strong interaction. This indicated that ZnO and LDPE did not have similar cohesive energies and their interaction is not expected. LDPE and LLDPE are very similar in chemical composition, the main difference being the shorter side chains of LLDPE than of LDPE. Thus, it can be concluded that ZnO and LLDPE are also not compatible with each other.

The water contact angle of surfaces also indicated the similarities of surfaces. The ZnO powders had low water contact angles (47, 45, and 38° for mZnO, sZnO, and nZnO, respectively). nZnO was the most hydrophilic filler. Since LLDPE was hydrophobic with 125° water contact angle as reported in Table II, it was not possible to prepare 20 vol % loaded composite from nZnO.

### Surface Roughness and Contact Angle of the ZnO and Polymer Composites

In general, the roughness of a surface can affect any contact angle measurement. The contact angle measurements of the pelletized ZnO powders, could not be made due to the high roughness and porous structure of the pellets. The smooth surface and nonporous structure was obtained for unmodified powders by sintering the pellets at 1100°C. The accuracy of the contact angle measurements usually attributed to the surface roughness of the measured material. According to Wenzel relation, as the surface roughness increases the contact angle for a water droplet on a hydrophobic surface also increases.<sup>28</sup> Thus both the ZnO pellets and composites films had very low surface roughness values as reported in Table I and II, respectively. Thus the contact angle measurements were not affected by the surface roughness. Water contact angle values and surface roughness of polymeric composites are given in Table II. The water contact angle (CA) of LLDPE was determined as  $125 \pm 5^\circ$ . This value is close to the value reported for low density polyethylene.<sup>29</sup> Addition of ZnO particles with a hydrophilic nature to LLDPE decreased the contact angle to around 89–91°.

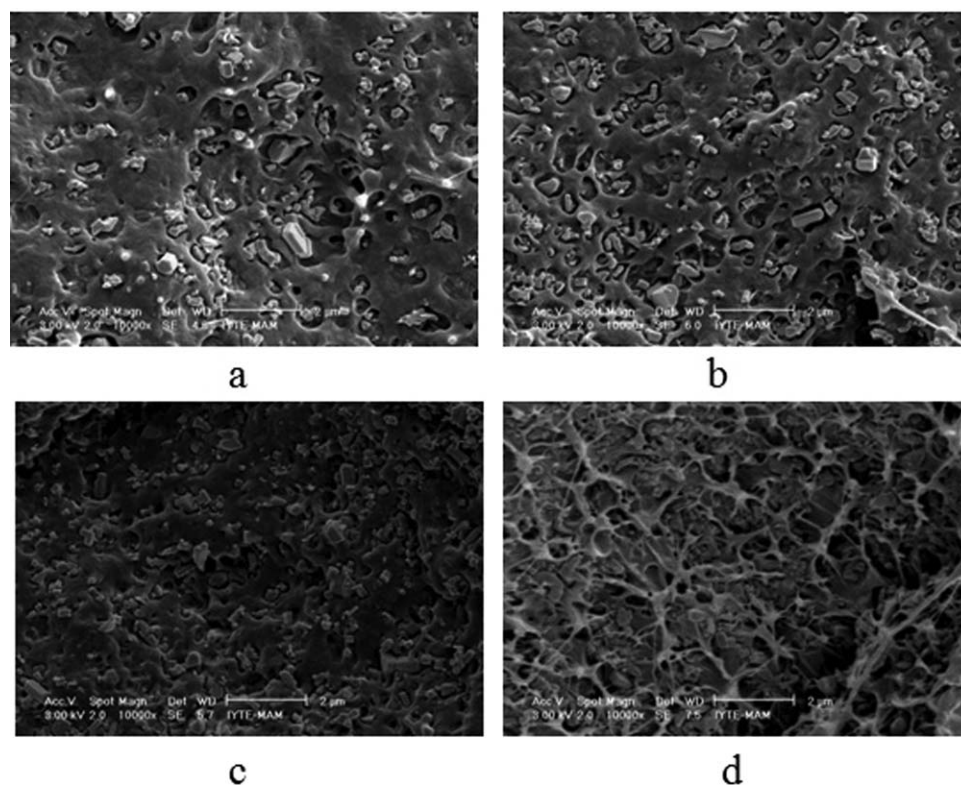


**Figure 4.** sZnO-LLDPE composites SEM micrographs for (a) 5 vol %, (b) 10 vol % (c) 15 vol %, and (d) 20 vol % sZnO.

### Mechanical Properties of the Composites

LLDPE matrix composites are flexible and ductile plastics which tend to be tough and resist deformation. The force elongation curves for mZnO filled composites are seen in Figure 5. The mechanical properties of composites were significantly influenced by the addition of ZnO powder, since their yield stress, elastic modulus, tensile strength, and elongation at break changed as shown in Figures 6–9. ZnO addition to the polymer matrix decreased the toughness, increased the brittleness, and stiffness. The yield stress of the composites filled with mZnO slightly increased with vol % of filler due to needle shape of the particles. However, yield stress decreased from 8.3 MPa down to 5.3 MPa as the nZnO loading increased up to 15% (Figure 6). Elastic modulus of nanosized ZnO particles loaded composites was found to be higher than that of the micron sized ZnO loaded ones (Figure 7). This might be due to the smaller size of the agglomerates for nZnO than mZnO in composites. As the vol % of the filler increases the Young modulus increases more

**Table II.** The Surface Roughness and the Contact Angle of Water on the Surface of the Composites

ZnO type	Volume % of ZnO	Contact angle (°)	Surface roughness ( $\mu\text{m}$ )
Non	0	125	0.09
mZnO	15	89	0.1
sZnO	15	90	0.09
nZnO	15	91	1.38

for the nZnO composites than mZnO composites. Stiffness of the composites prepared by nZnO having nano particle size increased more compared to composites with micron sized ZnO. By increasing the filler content, nZnO loaded composite changed from plastic to brittle structure.

The ultimate elongation of pure LLDPE was very high, but with the addition of ZnO to the composite the ultimate elongation was decreased for ZnO particles with micron and nanosizes as shown in Figure 9.

Previous studies showed that when nano ZnO was added at low concentrations (0.3%) the tensile strength and elongation at

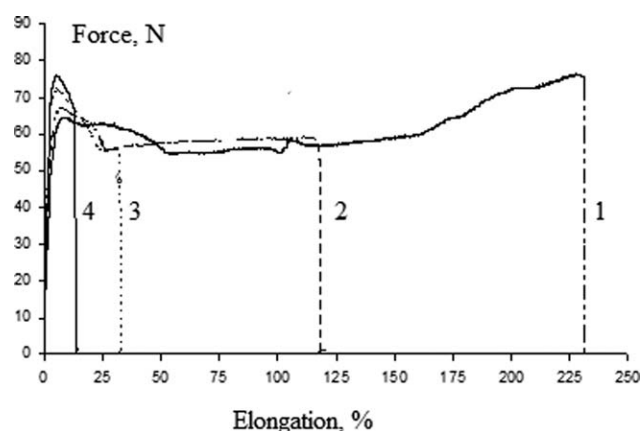


**Figure 5.** Force elongation curves for (1) LLDPE, composites having (2) 5 vol %, (b) 10 vol %, (c) 15 vol %, and (d) 20 vol % mZnO.

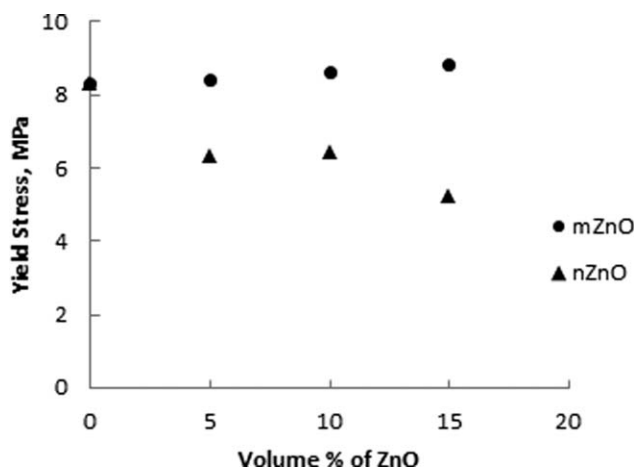


Figure 6. Change of yield stress of the composites with vol % ZnO.

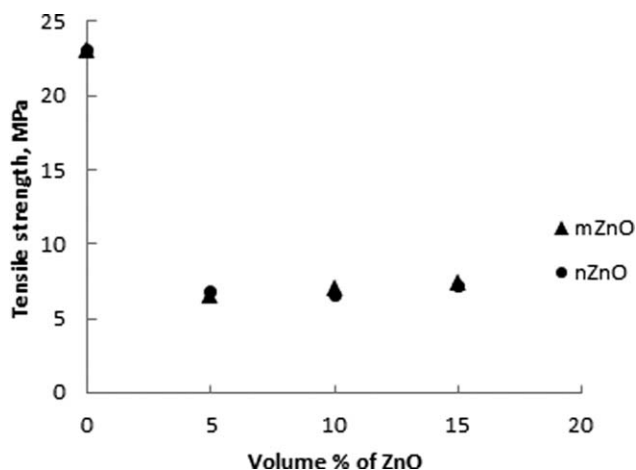


Figure 8. Change of the tensile strength of the composites with vol % of ZnO.

break increased by 43.2 and 39.4%, respectively.<sup>30</sup> However incorporating particles at a high concentration to the LLDPE matrix reduces chains mobility which leads to a rapid decrease in elongation at break, and introduces discontinuity in stress transfer to the filler–polymer interface in the composites structure as observed in this study.

In spite of having relatively low yield stress, both composites can be used as engineering materials since they can safely be loaded up to 8.4 and 5.2 MPa stress for mZnO–LLDPE and nZnO–LLDPE, respectively.

### The Electrical Resistivity of Composites

The electrical resistivity of the composites will be simultaneously affected from the initial resistivity values of the ZnO fillers, even distribution of fillers in the composites and the presence of empty space at the interface of ZnO and polymer. The voids (gaps) observed in composites (Figure 4) inhibited the conduction of electrons in the composites. However, due to the conductive path created by touching of the ZnO particles, the overall conductivity increased with ZnO addition. The volume resistivity values of composites are given in Figure 10. The materials should have an electrical conductivity in the range of

$10^{12}$  and  $10^8 \Omega \text{ cm}$  for ESD applications,  $10^8$  and  $10^2 \Omega \text{ cm}$  for moderately conductive applications and  $10^2 \Omega \text{ cm}$  and higher for shielding applications. According to this information, the composites which had 20 vol % sZnO and mZnO and 15 vol % for nZnO could be used in ESD applications. Especially, mZnO–LLDPE composites were 100 times more conductive than composites prepared from other powders at 20 and 15 vol % loading.

The crystallinity of the composites were higher than the LLDPE. Since the electron flow through amorphous parts could enhance the conductivity of ZnO–LLDPE, the conductivity of the composites having higher crystallinity should have been lower than the pure polymer matrix. However, the reverse case was observed and the conductivity was increased with volume fraction of the filler. Thus, the conductivity change in composites was not related to the crystallinity. It was more related to the initial electrical conductivity of the filler and aspect ratio of the filler.

Theoretically, increasing the surface area might increase the probability of the touching of the particles. According to general effective media theory, the conductor–insulator relation was explained by percolation. In percolation effect, there should be a conductive path which is based on zinc oxide.

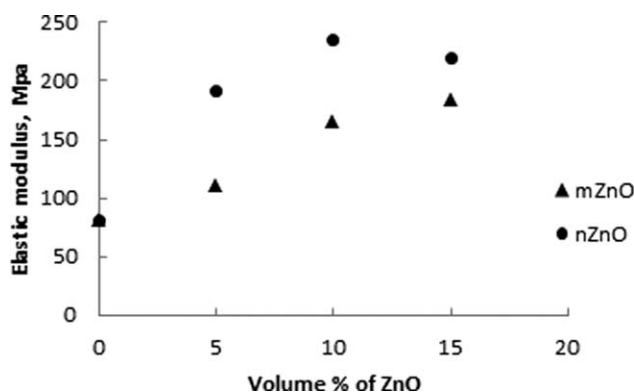


Figure 7. Change of the elastic modulus of the composites with vol % of ZnO.

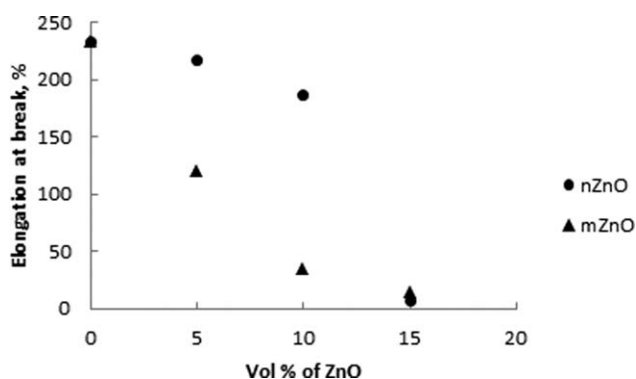


Figure 9. Elongation at break of the composites with vol % of ZnO.

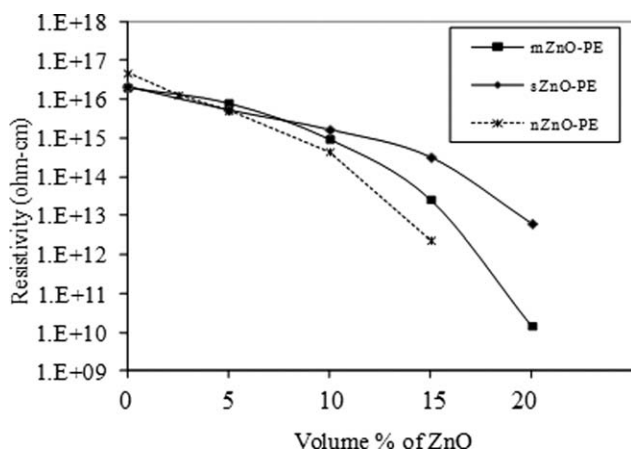


Figure 10. Change of resistivity of composites with vol % of ZnO.

When the concentration of filler is at or above the percolation threshold value, the resistivity of the composites will decrease dramatically. However, only mZnO loaded composites resistivity value decreased dramatically to  $1.4 \times 10^{10} \Omega \text{ cm}$  from  $2.3 \times 10^{16}$  with increasing filler content. This could be due to initial low resistivity of mZnO and high aspect ratio of mZnO powder. According to Hong et al.<sup>19</sup> and Tjong et al.,<sup>31</sup> the electrical resistivity values of ZnO-PE composites were  $10^9 \Omega \text{ cm}$  after 30 vol % addition of ZnO and  $10^{13} \Omega \text{ cm}$ , after the addition of 60 vol % ZnO addition respectively. If the results of this study were compared with the related papers, in this study, the lowest electrical resistivity was found as  $10^{10} \Omega \text{ cm}$  for 20 vol % mZnO composite.

**Effect of Interparticle Distance on Electrical Resistivity.** Hong et al.<sup>19</sup> predicted the interparticle distance of spherical particles with uniform size distribution in composites using eq. (2).

$$l = r \left[ \frac{4\pi}{3\Phi} \right]^{1/3} - 2 \quad (2)$$

Where  $r$  is the radius of the particle and  $\Phi$  is the volume fraction of the filler in the composite.<sup>19</sup> The assumptions for using this equation was that they are homogeneously dispersed, uniformly distributed spherical particles in a polymeric network. The assumptions about the particle shape and uniform size distribution could not be justified, since the particle sizes were generally polydisperse and there were no uniform distribution of the particles in the composites. Interparticle distances between particles were calculated for all composites and their relations with the resistivity of the composites were investigated. Figure 11 shows the natural logarithm of the resistivity of the composites versus interparticle distance. Although the expectations was that there would be a decrease in electrical resistivity by decreasing interparticle distance,<sup>19,31</sup> mZnO powders having the highest interparticle distance had the lowest resistivity. In the case of ZnO having different particle size with identical electrical resistivity, the results could be compared with the interparticle distances reported by Hong et al.<sup>19</sup> However, each ZnO

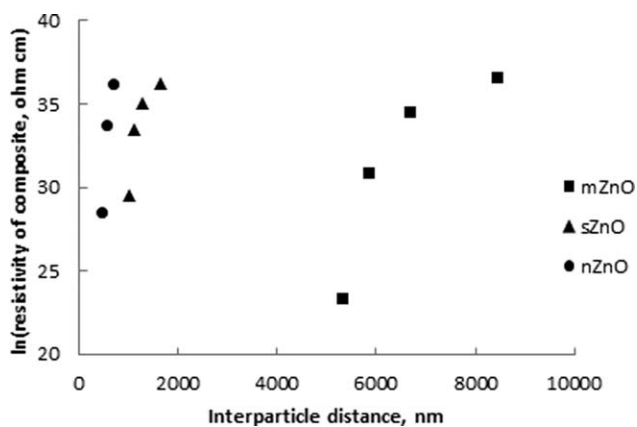


Figure 11. Change of the natural logarithm of resistivities of composites versus interparticle distance.

powder used in this study had a different resistivity value, thus the comparison could not be made.

**Effect of Initial Resistivity of Zinc Oxide on Resistivity of Composites.** The relation of the electrical resistivity of composites with the initial resistivity of zinc oxide powders was also investigated. The natural logarithm of the resistivity of the composites versus initial resistivity of ZnO powders at constant filler loadings is shown in Figure 12. At low levels of loading, the resistivity of the composite is close to the resistivity of the matrix polymer, but at high loading levels, the resistivity is the smallest for mZnO having the smallest initial resistivity.

**Effect of the aspect Ratio of the Filler on the Resistivity.** The aspect ratio of the filler also affected the resistivity of the composites. In Figure 13, the resistivity of the composites is low for the highest aspect ratio for high filler loadings.

These composites could be used as an antistatic material or in moderately conductive applications in electronics industry since they have resistivity values at the order of  $10^{-13}$  to  $10^{-10}$ .

#### The Thermal Conductivity of the Composites

The thermal conductivity of the composites increases with increasing zinc oxide content as shown in the Figure 14. At the

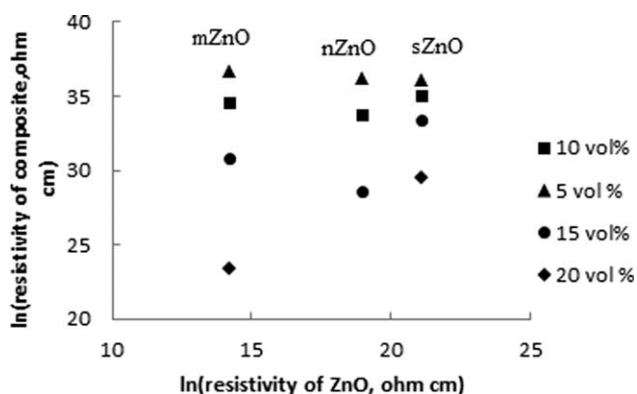
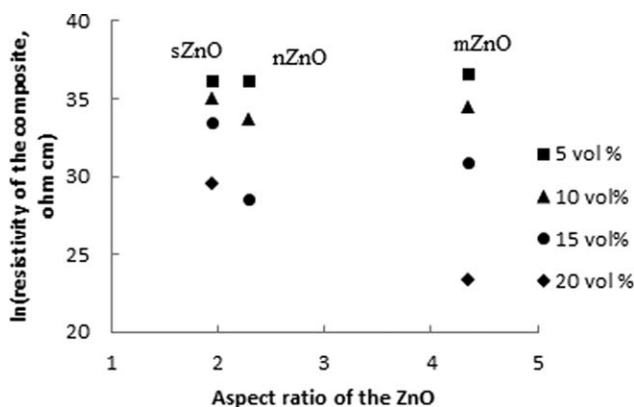


Figure 12. Change of the natural logarithm of resistivities of composites versus logarithm of initial resistivities of the ZnO powders.





**Figure 13.** Change of the natural logarithm of resistivities of composites versus the aspect ratio of the ZnO powders.

same loading level, the conductivity values for LLDPE composites followed the order as mZnO, sZnO, and nZnO. Interfaces between materials become increasingly important on small length scales. For sufficiently small particles, the properties of the polymer/particle interface also control thermal transport in the composite. However, in this study, the big agglomerates obtained from nanoparticles in the composites during the fabrication.

LLDPE is a dielectric material; therefore, the thermal conduction is transport but by phonons.<sup>21</sup> The semi-crystalline polymer allows for the better conduction of phonons with less scattering incidents than that of an amorphous material so crystallinity of the polymer is very important. A 20 vol % loaded mZnO has the highest thermal conductivity, it could be due to the aspect ratio of the filler since the transport mechanism explained by phonons by exciting one or more atoms by twisting, pulling, or pushing will be easily propagate the transportation of energy. The thermal conductivity was affected most by the addition of 20 vol % of mZnO and sZnO to LLDPE composites and it was found 1.56 and 1.26 W/mK. The conductivity of the composites were increased about 2.5–3 times for the highest loading compared to polymer's thermal conductivity. The sZnO and mZnO loaded composites can be used in heat sink applications.

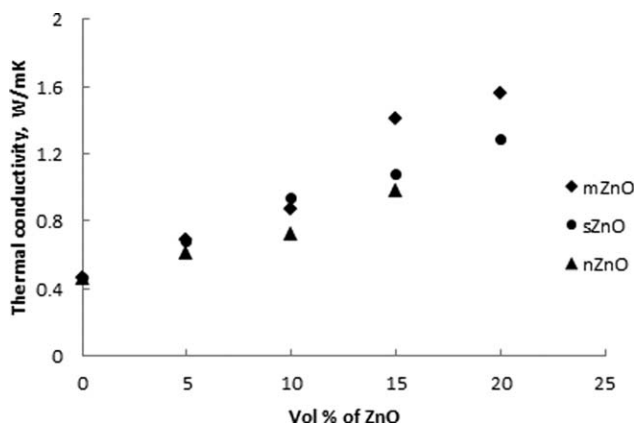


**Figure 14.** Change of the thermal conductivity with vol % of ZnO in composites.

## CONCLUSIONS

The effects of different particle sized ZnO fillers having different initial resistivities on the electrical and thermal behavior of LLDPE nanocomposites were investigated by measuring the electrical resistivity and thermal conductivity of the composites. The contact angle of water indicated that ZnO powders were hydrophilic and LLDPE was hydrophobic. Rather than the particle size of the ZnO, its initial resistivity and aspect ratio affected the resistivity of composites. The ZnO addition to the polymer matrix decreased the toughness, increased the brittleness and stiffness. The resistivity of PE matrix was  $10^{16}$   $\Omega$  cm and it decreased to  $10^{10}$   $\Omega$  cm after addition of 20 vol % mZnO filler. Generally, the highest loadings of ZnO created the highest conductivities in the composites. The thermal conductivity of the composites was increased 2.5- to 3-fold by ZnO addition up to 20 vol %. The thermal conductivity was increased most for mZnO composite to 1.56 W/mK.

In spite of having relatively low yield stress, the LLDPE–ZnO composites can be used as an engineering material in electrostatically dissipating, coating, and heat sink applications.

## ACKNOWLEDGMENTS

The authors acknowledge the financial support of this project with project number İYTE BAP 2006 İYTE 25.

## REFERENCES

- Sethi, R. S.; Goosey, M. T. In *Special Polymers for Electronics & Optoelectronics*; Chilton, J. A., Goosey, M. T., Eds.; Chapman & Hall: London, **1995**, pp 14–46.
- Grob, M. C.; Minder, E. *Plast. Addit. Comp.* **1999**, *1*, 20.
- Gojny, F. H.; Wichmann, M. H. G.; Fiedler, B.; Kinloch, I. A.; Bauhofer, W.; Windle, A. H.; Schulte, K. *Polymer* **2006**, *47*, 2036.
- Gubin, S. P. *Colloids Surf. A: Physicochem. Eng. Asp.* **2002**, *202*, 155.
- Wang, Z. L. *J. Phys.: Condensed Matter*. **2004**, *16*, 829.
- Tang, E.; Tian, B.; Zheng, E.; Fu, C.; Cheng, G. *Chem. Eng. Commun.* **2008**, *195*, 479.
- Gokturk, H. S.; Fiske, T. J.; Kalyon, D. M. *ANTEC* **1992**, p 491.
- Clingermaun, M. L. *Development and Modeling of Electrically Conductive Composite Materials*; Ph.D. thesis, **2001**.
- Mamunya, Ye. P.; Zoisb, H.; Apekis, L.; Lebedev, E. V. *Powder Technol.* **2004**, *140*, 49.
- Sun, J.; Gokturk, H. S.; Kalyon, D. M. *J. Mater. Sci.* **1993**, *28*, 364.
- Bigg, D. M. *Polym. Eng. Sci.* **1977**, *17*, 842.
- Taya, M. *Electronic Composites Modeling, Characterization, Processing and Mems Applications*; Cambridge University Press: Cambridge, **2005**, pp 1–11.
- Kalaitzidou, K.; Fukushima, H.; Drzal, L. T. *Materials*. **2010**, *3*, 1089.
- Lux, F. J. *Mater. Sci.* **1993**, *28*, 285.

15. Gokturk, H. S.; Fiske, T. J.; Kalyon, D. M. *J. Appl. Polym. Sci.* **1993**, *50*, 1891.
16. Krueger, Q. J. Master Thesis, Michigan Technological University, **2002**.
17. Tchoudakov, W. J. R.; Breier, O.; Narkis, M.; Siegmann, A. *Polym. Eng. Sci.* **1996**, *36*, 1336.
18. Hong, J. I.; Schadler, L. S.; Siegel, R. W.; Martensson, E. *Appl. Phys. Lett.* **2003**, *82*, 1956.
19. Hong, J. I.; Schadler, A. L. S. A.; Siegel, R.; Martensson, E. *J. Mater. Sci.* **2006**, *41*, 5810.
20. Fleming, R. J.; Ammala, A.; Casey, P. S.; Lang, S. B. *IEEE Trans. Dielectrics Elec. Insulation* **2008**, *15*, 118.
21. Weber, M.; Kamal, M. R. *Polym. Compos.* **1997**, *18*, 711.
22. Kumlutaş, D.; Tavman, I. H. A. *J. Thermoplast. Compos. Mater.* **2006**, *19*, 441.
23. Liufu, S.; Xiao, H.; Li, Y. *Powder Technol.* **2004**, *145*, 20.
24. Krupa, I.; Novek, I.; Chodak, I. *Synth. Metals* **2004**, *145*, 245.
25. JCPDS Card No.: 79-0207.
26. Shafiq, M.; Yasin, T.; Saeed, S. *J. Appl. Polym. Sci.* **2011**, *123*, 1718.
27. Hansen, C. M. *Hansen Solubility Parameters: A User's Handbook*; CRC Press: New York, **2007**.
28. Hsieha, C.; Chena, J.; Kuo, R.; Lin, T.; Wu, C. *Appl. Surf. Sci.* **2005**, *240*, 318.
29. Gilliam, M. A.; Yu, Q. S. *J. Appl. Polym. Sci.* **2006**, *99*, 2528.
30. Li, S.; Li, B.; Qin, Z. *Polym. Plast. Technol. Eng.* **2010**, *49*, 1334.
31. Tjong, S. C.; Liang, G. D. *Mater. Chem. Phys.* **2006**, *100*, 1–5.